Available online at www.sciencedirect.com
SCIENCE DIRECT
Journal of Pharmaceutical and Biomedical Analysis 41 (2006) 500–509
JOURNAL OF PHARMACEUTICAL AND BIOMEDICAL ANALYSIS
www.elsevier.com/locate/jpba

Distribution and metabolism of the antipsychotic agent mazapertine succinate in rats

Gary W. Caldwell *, Wu-Nan Wu, Linda A. McKown, A. Diane Gauthier, John A. Masucci, William J. Jones, Gregory C. Leo, Allen B. Reitz

Johnson & Johnson Pharmaceutical Research and Development, L.L.C., Spring House, PA 19477, USA

Received 19 April 2005; received in revised form 20 October 2005; accepted 21 October 2005
Available online 28 December 2005

Abstract

The pharmacokinetics and drug disposition of ^{14}C 1-[3-[[4-[2-(1-methylethoxy)phenyl]-1-piperazinyl]methyl]benzoy]piperidine succinate (RWJ-37796, mazapertine, Mz) have been investigated in male and female Sprague–Dawley rats. Approximately 93% of the orally administered radioactive dose (30 mg/kg) was recovered after 7 days. Fecal elimination accounted for approximately 63% of the dose while urine accounted for 30%. The rate of elimination of ^{14}C Mz was rapid with 81% of the total fecal and 94% of the total urinary radioactivity being excreted within 24 h. There were no significant gender differences in the overall excretion pattern. The maximal plasma concentration of Mz and total radioactivity occurred at 0.5 h after dosing and plasma concentrations were consistently higher in female rats. The Mz concentration declined rapidly in plasma with a terminal half-life <2 h. The total radioactive dose in plasma displayed a considerably longer terminal half-life of 9–13 h. Mz and a total of 15 metabolites were isolated and identified in these samples. Unchanged Mz accounted for <5% of the radioactive dose in excreta samples and <8% of the sample in plasma (0–24 h). Metabolites were formed by phenyl hydroxylation, piperidyl oxidation, *O*-dealkylation, *N*-dephenylation, oxidative *N*-debenzylation and glucuronide conjugation.

Keywords: Rats; Pharmacokinetics; Excretion; Metabolism; 1-[3-[[4-[2-(1-Methylethoxy)phenyl]-1-piperazinyl]methyl]benzoy]piperidine succinate; RWJ-37796; Mazapertine

1. Introduction

Mazapertine (1-[3-[[4-[2-(1-methylethoxy)phenyl]-1-piperazinyl]methyl]benzoy]piperidine succinate, RWJ-37796, Mz) has been shown to be an effective antipsychotic agent which binds with high affinity to D_2, D_3, 5-HT_{1A} and α_{1A}-adrenergic receptors [1–3]. Preliminary results on the psychopharmacological profile and pharmacokinetics of Mz in healthy male volunteers have been reported [4,5]. These abstracts indicated that Mz was well absorbed and extensively metabolized in healthy males. After a single oral dose of Mz (40 mg/kg), 10 metabolites were tentatively identified in urine using liquid chromatography mass spectrometry (LC/MS) methods. The in vitro metabolism of Mz has been investigated in rat hepatic 9000 g supernatant (S9) [6]. Mz was metabolized to 12 metabolites in rat hepatic S9 fraction with the major in vitro biotransformation pathways involving *O*-dealkylation and oxidation at the phenyl and piperidyl rings. The drug disposition of radiolabeled ^{14}C Mz in dogs has been investigated [7]. Mz was well absorbed and extensively metabolized in beagle dogs with 14 metabolites being isolated and identified by LC/MS methods. These metabolites accounted for >60% of the dose radioactivity in plasma, 17% in urine, and 28% in feces. The major in vivo biotransformation pathways in beagle dogs involved oxidation at the phenyl and piperidyl rings, oxidative *N*-debenzylation and depiperidylation. Many of the metabolites that were identified in this in vivo dog study were structurally identical (i.e. LC/MS/MS data) to those in the in vitro rat and in vivo human studies [8]. Several of the key metabolites of Mz have been synthesized [9,10].

Due to the importance of orally active benzamide antipsychotic agents, such as Mz, the present work provides full details for the excretion and metabolism of ^{14}C Mz in Sprague–Dawley

* Corresponding author at: Johnson & Johnson Pharmaceutical, Research and Development, Welsh & McKean Roads, P.O. Box 776, Spring House, PA 19477, USA. Tel.: +1 215 628 5537; fax: +1 215 628 7064.
E-mail address: gcaldwel@prius.jnj.com (G.W. Caldwell).

0731-7085/$ – see front matter © 2005 Elsevier B.V. All rights reserved.
doi:10.1016/j.jpba.2005.10.052

rats. We report the isolation and identification of Mz and a total of 15 metabolites using a variety of chromatographic methods, nuclear magnetic resonance (NMR), mass spectrometry (MS), methyl derivatization, and glucuronic hydrolysis techniques. The excretion of Mz and these metabolites in plasma, urine and feces are discussed along with the key pharmacokinetic parameters.

2. Experimental

2.1. Materials

^{14}C Mz, Mz [1], metabolite M1 (RWJ-50503) [9], metabolite M2 (RWJ-48772) [9], metabolite M4 (RWJ-50292) [9], metabolite M7 (RWJ-47999) [9], M11 (RWJ-48278) [9] and metabolite M14 (RWJ-380037) [9] were synthesized at Johnson & Johnson Pharmaceutical Research and Development L.L.C. (Spring House, PA, USA). The radiochemical purity of ^{14}C Mz and unlabeled purity of Mz, M1, M2, M4, M7, M11 and M14 were shown to be >98% by TLC and HPLC (data not shown). The position of the ^{14}C labeling in Mz was at the carbonyl carbon. Vacutainers® and Venoject® (heparinized tubes) were purchased from Becton-Dickinson & Co. (Franklin Lakes, NJ, USA). XAD-2 Amberlite® resin was obtained from Rohm & Haas (Philadelphia, PA, USA). Glusulase®, a mixture of arylsulfatase and β-glucuronidase (1:4 v/v) from *Helix pomatia*, was obtained from Endo Laboratories Inc. (Wilmington, DE, USA). Diazald® (diazomethane reagent) was obtained from Aldrich Chemical Co. (Milwaukee, WI, USA). Biofluor®, used as a scintillation solution, was purchased from New England Nuclear (Boston, MA, USA). HPLC grade solvents were purchased from the Fisher Scientific Co. (Fair Lawn, NJ, USA) and glass-distilled solvents were from Burdick and Jackson Laboratories Inc. (Muskegon, MI, USA). Other reagent chemicals were from commercial sources and used without further purification.

2.2. Rat study

Twenty-two male and 22 female Sprague–Dawley rats (Charles River Breeding Labs., Kingston, NY, USA) weighing between 0.19 and 0.24 kg were used in this study. Rats were housed one rat per cage in a rodent room where the lighting was on a 12 h light/12 h dark cycle. The rodent room was maintained between 18–26 °C and 30–70% humidity. Rats were fed laboratory Lab-Blox (Purina Mills, St. Louis, MO, USA). The rats were fasted 18 h prior to dosing and their normal feeding (food and water ad libitum) schedule was resumed immediately after dosing.

The radiolabeled oral dose was prepared by dissolving 320 mg of ^{14}C Mz in 64 mL of distilled water. The final concentration of the solution was 5 mg/mL at 12.93 μCi/mg. This concentration (i.e. the expected therapeutic dose) was selected to match an earlier 3-month toxicity study. Depending on their weight, the rats each received between 1.14 and 1.44 mL of ^{14}C Mz by an oral gavage needle. Thus, the rats received a single oral dose of 30 mg/kg of ^{14}C Mz. Rats were randomly assigned to excretion (Table 1; 4M/4F) and blood (Table 2, Fig. 1; 16M/16F) (Table 2) collection groups. At pre-selected times after dosing (0.5, 1, 2, 4, 6, 8, 12 and 24 h), blood samples (ca. 8 mL) were collected, from the blood collection group, via cardiac puncture into heparinized tubes after the rats were anesthetized with carbon dioxide gas. The blood samples were centrifuged for 20 min at 2000 rpm at 10 °C to obtain plasma. Plasma samples were stored in glass screw-cap test tubes at about −20 °C until analysis. Urine and fecal sample extracts were collected at 24 h intervals for 5 days followed by an additional 48 h collection

Table 1
Percent of total ^{14}C recovered and percent of dose represented by mazapertine (RWJ-37796, Mz) and its metabolites in plasma, urine fecal samples[a]

Sample	Plasma	Urine	Feces
Pooled sample	(0.5–24 h)	(0–24 h)	(0–24 h)
Sex	M	M	M
Dose	30 mg/kg	30 mg/kg	30 mg/kg
%Dose	NA	29	57
Mz	8	+	+
M1	–	+	34
M2	29	5	7
M3	–	5	10
M4	17	+	+
M5	–	+	10
M6	–	13	11
M7	+	15	+
M8	–	+	–
M9	–	–	+
M10	–	+	–
M11	21	30	–
M12	+	10	–
M13	–	+	–
M14	–	+	–
M15	–	+	–
%Sample[b]	>80	>87	>85

[a] See Section 3 for description of table results. Plus sign denotes <5% of total in sample. Negative sign denoted metabolite not detected. NA denoted not available. See Fig. 3 for structure of Mz and metabolites.
[b] Total ^{14}C in sample (Mz plus metabolites) identified.

Table 2
Summary of excretion and pharmacokinetic parameters of ^{14}C mazapertine (RWJ-37796, Mz) in males and females rats

Parameter	Males	Females
%Total dose recovered[a]	95.0 ± 1.9%	90.1 ± 4.4%
%Dose in urine[a]	30.1 ± 1.1%	29.8 ± 3.0%
%Dose in feces[a]	64.9 ± 2.5%	60.3 ± 7.2%
C_{max} (total radioactivity)[b]	5987 ng equiv./mL	8846 ng equiv./mL
C_{max} (mazapertine)[b]	179 ng equiv./mL	1263 ng equiv./mL
AUC (total radioactivity)[c]	13929 ng equiv. h/mL	28280 ng equiv. h/mL
AUC (mazapertine)[c]	264 ng equiv. h/mL	2310 ng equiv. h/mL
$t_{1/2}$ (total radioactivity)[d]	13.0 h	8.6 h
$t_{1/2}$ (mazapertine)[d]	1.1 h	1.5 h

[a] Samples collected for 7 days with $N = 4$ rats/sex.
[b] Maximum concentration for $N = 2$ rats/sex.
[c] AUC denotes area under the plasma curve from 0 to 24 h. The AUC was calculated from 2 rats/sex and 8 time points (Fig. 1).
[d] Half-life calculated from terminal phase of mean plasma concentration data (Fig. 1).

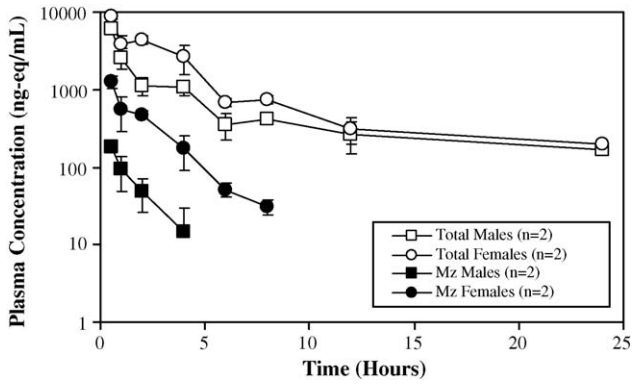

Fig. 1. Mean plasma concentration of the total radioactivity and mazapertine in male and female rats following oral administration of ^{14}C mazapertine (30 mg/kg).

interval in cooled plastic bottles following dose administration. These samples were transferred to polypropylene screw-cap tubes and stored at about −20 °C until purification and analysis.

2.3. Radioactivity determination

Duplicate aliquots (0.1 mL) of plasma and triplicate aliquots of urine and fecal extracts (0.1–1.0 mL) were assayed for total radioactivity in 10 mL of Biofluor® by liquid scintillation spectrometry (Tables 1–3). Plasma, urine, and fecal extract pools were prepared for metabolite isolation and identification. The total radioactivity contained in each sample pool, before and after purification, was also determined by direct liquid scintillation counting. Feces residue (300 mg per aliquot) was analyzed in triplicate by combustion. ^{14}C-labeled carbon dioxide formed was trapped with a PerafluorV/Carbosorb-CO_2 (3:2 v/v) mixture and analyzed by a Beckman 3801 Liquid Scintillation Counting System purchased from Beckman Instruments (Fullerton, CA, USA).

2.4. Chromatography

Selected samples were pooled and analyzed by TLC and HPLC for biotransformation profiling. Prior to chromatographic analysis, it was necessary to purify most of the samples. The plasma samples were pooled, lyophilized, extracted with methanol, evaporated to dryness and reconstituted with methanol. The radioactivity profiles of the plasma samples were comparable before and after purification. The percentage of radioactivity recovered following purification of plasma samples was >95%. The urine samples were pooled, stirred with XAD-2 Amberlite® resin and filtered. The filtrate was washed with water, extracted with methanol, evaporated to dryness and reconstituted with methanol. The percentage of radioactivity recovered following purification of urine samples using this method was >95%. The fecal samples were pooled, evaporated to dryness, extracted with 5% acetic acid, evaporated and reconstituted with methanol. The percentage of radioactivity recovered following purification was 100%.

TLC analysis of the samples was performed using the following basic solvent system: methylene chloride/methanol/ammonium hydroxide (93/3.5/0.5 v/v/v). Each TLC plate was developed to a height of 14 cm above the spot or band where the sample was originally applied. Each sample was co-chromatographed with Mz, M1, M2, M4, M7, M11 and M14 as reference compounds, which were visualized by UV light after each plate was air-dried (data not shown). Each plate was also analyzed utilizing a RTLC scanner radiochromatogram imaging system (Radiomatic Instrument and Chemical Co., Tampa, FL, USA).

HPLC analysis of each sample pool (50–100 μL injected) was performed using the following gradient elution method. Solvent A was water containing 0.2% ammonium acetate, while solvent B was methanol containing the same percentage of buffer. The gradient program was carried out from 0% B to 100% B in 20 min and a hold time for 10 min at 100% B at a flow rate of 1 mL/min. All ^{14}C tracings were obtained using an on-line radioactivity flow detector (data not shown). The limit of detection for Mz in plasma was approximately 2 ng equiv./mL.

2.5. Analytical

Thin-layer radiochemical analyses were performed using 5 cm × 20 cm silica gel GF plates (250 μm gel thickness; Analtech Inc., Newark, DE, USA). TLC plates were analyzed using a radiochromatogram imaging system (BID100) (Bioscan Inc., Washington, DC, USA). The HPLC used was a gradient liquid chromatograph (Beckman Instruments, Fullerton, CA, USA) connected to a radioactivity flow detector (IN/US Service Corp., Fairfield, NJ, USA). LiChrosorb RP-18 MPLC guard and analytical columns (10 μm, 10 mm × 4.6 mm i.d.) were used for sample analysis (Brownlee Labs. Inc., Santa Clara, CA, USA).

Direct chemical ionization (DCI) and electron ionization (EI) mass spectra were obtained utilizing a VG7070E (VG Micromass, Manchester, UK) where the operating conditions for the spectrometer were as follows: source temperature at 200 °C; ionization potential at 70 eV; multiplier voltage at 1.8 keV; electrometer setting at 10^{-7} A/V; reagent gas was methane; mass range *m/z* 100–1000 Da. Fast atom bombardment (FAB) mass spectra were obtained on a VG7070E. A resolution of 1000 (10% valley definition) was used to record all spectra over a mass range of *m/z* 18–1000 Da. The mass spectrometer was scanned exponentially down using a scan rate of 1 s per decade. An Ion Tech Saddlefield gun, which generated a primary beam of argon atoms at 8 keV and 2 mA, was used for the FAB analysis. Thioglycerol was used as the FAB matrix.

Proton (^{1}H) NMR spectra were obtained on a Bruker AM-400 Fourier transform spectrometer equipped with an Aspect 3000 data system. Typical ^{1}H NMR spectra were obtained using a pulse width of 3 μs (30°); a 1 s recycling delay; 100 transients processed with a 0.1 Hz exponential weighting function and a spectral width of 8064 Hz over 32,768 complex data points, resulting in a digital resolution of 0.5 Hz per point. The experimental temperature used for NMR data collection was 24 ± 1 °C. The estimated amount of metabolites was between 50

Table 3
Proton (^{1}H) NMR chemical shifts and MS fragments of mazapertine (Mz) and its metabolites

Species[a] (molecular weight, amu)	^{1}H NMR[b], 400 MHz, chemical shifts (δ) ppm (CH_3OH)	*m/z* [cation, % relative intensity]
Mazapertine (421)	7.45 [m, 3H, Ring C], 7.25 [d, 1H, Ring C], 6.90 [m, 4H, Ring A], 4.60 [m, 1H, OC*H*(Me)$_2$], 3.75 [br s, 2H, CONCH$_2$, Ring D], 3.60 [s, 2H, NCH$_2$Ar], 3.45 [br s, 2H, CONCH$_2$, Ring D], 3.10 [br s, 4H, Ring B], 2.65 [br s, 4H, Ring B], 1.75 [br s, 4H, Ring D], 1.55 [br s, 2H, Ring D], and 1.25 [d, 6H, (Me)$_2$]	DCI (CH_4): 422 [*M*H$^+$, 100%], and 450 [*M*C$_2$H$_5^+$, 10%]; EI: 421 [*M*$^+$, 10%], 257 [8%], 230 [45%], 202 [8%], 176 [20%], 164 [40%], 148 [24%], 132 [27%], 119 [100%] and 91 [55%]
M1 (437)	7.45 [m, 3H, Ring C], 7.25 [d, 1H, Ring C], 6.75 [d, 1H, Ring A], 6.40 [s, 1H, Ring A], 6.30 [d, 1H, Ring A], 4.60 [m, 1H, OCH(Me)$_2$], 3.75 [br s, 2H, CONCH$_2$, Ring D], 3.60 [s, 2H, NCH$_2$Ar], 3.45 [br s, 2H, CONCH$_2$, Ring D], 3.10 [br s, 4H, Ring B], 2.65 [br s, 4H, Ring B], 1.75 [br s, 4H, Ring D], 1.55 [br s, 2H, Ring D], and 1.25 [d, 6H, (Me)$_2$]	DCI (CH_4): 438 [*M*H$^+$, 100%], and 466 [*M*C$_2$H$_5^+$, 10%]; EI: 437 [*M*$^+$, 12%], 257 [7%], 230 [23%], 202 [9%], 192 [30%], 180 [43%], 150 [24%], 136 [43%], 119 [100%], and 91 [50%]
M2 (437)	7.45 [m, 3H, Ring C], 7.25 [d, 1H, Ring C], 6.90 [m, 4H, Ring A], 4.60 [m, 1H, OCH(Me)$_2$], 4.20 [m, 1H, OCH], 3.75 [br s, 2H, CONCH$_2$, Ring D], 3.90 [s, 2H, NCH$_2$Ar], 3.65 [br s, 2H, CONCH$_2$, Ring D], 3.10 [br s, 4H, Ring B], 2.65 [br s, 4H, Ring B], 1.95 [br s, 2H, Ring D], 1.60 [br s, 2H, Ring D], and 1.25 [d, 6H, (Me)$_2$]	DCI (CH_4): 438 [*M*H$^+$, 100%], 466 [*M*C$_2$H$_5^+$, 15%], and 420 [*M*H$^+$ − H$_2$O 40%]; EI: 437 [*M*$^+$, 6%], 273 [9%], 246 [35%], 218 [10%], 176 [22%], 164 [37%], 148 [22%], 134 [33%], 119 [100%] and 91 [67%]
M3 (453)	7.45 [m, 3H, Ring C], 7.25 [d, 1H, Ring C], 6.75 [d, 1H, Ring A], 6.40 [s, 1H, Ring A], 6.30 [d, 1H, Ring A], 4.60 [m, 1H, OCH(Me)$_2$], 4.20 [br s, 1H, CONCH$_2$, Ring D], 3.85 [br s, 2H, CONCH$_2$, Ring D], 3.60 [s, 2H, NCH$_2$Ar], 3.10 [br s, 4H, Ring B], 2.65 [br s, 4H, Ring B], and 1.25 [d, 6H, (Me)$_2$]	DCI (CH_4): 454 [*M*H$^+$, 100%], 482 [*M*C$_2$H$_5^+$, 10%], and 438 [*M*H$^+$ − H$_2$O, 10%]; EI: 453 [*M*$^+$, 12%], 246 [15%], 218 [5%], 192 [30%], 180 [43%], 150 [50%], 134 [44%], 119 [100%] and 91 [56%]
M4 (379)	7.55 [m, 3H, Ring C], 7.45 [d, 1H, Ring C], 7.10 [m, 1H, Ring A], 6.90 [m, 1H, Ring A], 6.80 [m, 1H, Ring A], 3.70 [br s, 2H, CONCH$_2$, Ring D], 3.65 [s, 2H, NCH$_2$Ar], 3.40 [br s, 2H, CONCH$_2$, Ring D], 3.05 [br s, 4H, Ring B], 2.65 [br s, 4H, Ring B], 1.75 [br s, 4H, Ring D], and 1.55 [br s, 2H, Ring D]	DCI (CH_4): 380 [*M*H$^+$, 20%], and 119 [100%]; EI: 379 [*M*$^+$, 3%], 257 [5%], 245 [25%], 230 [18%], 202 [20%], 134 [94%], 122 [27%], 119 [100%] and 91 [85%]
M5 (555) = (379 + Glu)	7.60 [d, 1H, Ring A], 7.45 [m, 3H, Ring C], 7.30 [d, 1H, Ring C], 7.10 [m, 1H, Ring A], 6.90 [m, 1H, Ring A], 3.70 [br s, 2H, CONCH$_2$, Ring D], 3.65 [s, 2H, NCH$_2$Ar], 3.40 [br s, 2H, CONCH$_2$, Ring D], 3.15 [br s, 4H, Ring B], 2.70 [br s, 4H, Ring B], 1.65 [br s, 4H, Ring D], and 1.55 [br s, 2H, Ring D]	DCI (CH_4): 380 [*M*H$^+$, 100%], and 408 [*M*C$_2$H$_5^+$, 10%]; EI: 379 [*M*$^+$, 8%], 257 [5%], 245 [20%], 230 [20%], 202 [23%], 134 [70%], 122 [27%], 119 [100%] and 91 [80%] (sample decomposed in MS to M4)
M6 (571) = (395 + Glu)	7.60 [d, 1H, Ring A], 7.45 [m, 3H, Ring C], 7.30 [d, 1H, Ring C], 7.10 [m, 1H, Ring A], 6.90 [m, 1H, Ring A], 3.80 [br s, 1H, CONCHO, Ring D], 3.65 [s, 2H, NCH$_2$Ar], 3.65 [br s, 2H, CONCH$_2$, Ring D], 3.15 [br s, 4H, Ring B], 2.65 [br s, 4H, Ring B], 1.80 [br s, 2H, Ring D], 1.60 [br s, 2H, Ring D], and 1.50 [br s, 2H, Ring D]	DCI (CH_4): 396 [*M*H$^+$, 100%], 424 [*M*C$_2$H$_5^+$, 20%], and 378 [*M*H$^+$ − H$_2$O 18%]; EI: 395 [*M*$^+$, 9%], 273 [5%], 261 [12%], 246 [10%], 218 [11%], 134 [80%], 122 [20%], 119 [100%] and 91 [80%] (sample decomposed in MS)
M7 (287)	7.55 [m, 3H, Ring C], 7.45 [d, 1H, Ring C], 3.90 [br s, 2H, CONCH$_2$, Ring D], 3.75 [s, 2H, NCH$_2$Ar], 3.60 [br s, 2H, CONCH$_2$, Ring D], 3.05 [br s, 4H, Ring B], 2.65 [br s, 4H, Ring B], 1.85 [br s, 4H, Ring D], and 1.70 [br s, 2H, Ring D]	DCI (CH_4): 288 [*M*H$^+$, 100%], and 316 [*M*C$_2$H$_5^+$, 20%]; EI: 287 [*M*$^+$, 5%], 245 [24%], 231 [4%], 203 [17%], 202 [15%], and, 119 [100%]
M8 (303)	7.45 [m, 3H, Ring C], 7.30 [d, 1H, Ring C], 3.85 [br s, 1H, CONCH$_2$, Ring D], 3.60 [br s, 2H, CONCH$_2$, Ring D], 3.55 [s, 2H, NCH$_2$Ar], 2.80 [br s, 4H, Ring B], 2.45 [br s, 4H, Ring B], 1.80 [br s, 2H, Ring D], 1.60 [br s, 2H, Ring D], and 1.50 [br s, 2H, Ring D]	DCI (CH_4): 304 [*M*H$^+$, 100%], 332 [*M*C$_2$H$_5^+$, 18%] and 286 [*M*H$^+$ − H$_2$O 25%]; EI: 303 [*M*$^+$, 6%], 261 [25%], 218 [10%], 148 [10%], and 119 [100%]
M9 (303)	7.45 [d, 1H, Ring C], 7.35 [s, 1H, Ring C], 7.30 [d, 1H, Ring C], 3.65 [br s, 2H, CONCH$_2$, Ring D], 3.50 [s, 2H, NCH$_2$Ar], 3.45 [br s, 2H, CONCH$_2$, Ring D], 2.80 [br s, 4H, Ring B], 2.40 [br s, 4H, Ring B], 1.60 [br s, 4H, Ring D], and 1.50 [br s, 2H, Ring D]	DCI (CH_4): 304 [*M*H$^+$, 100%], 332 [*M*C$_2$H$_5^+$, 18%] and 286 [*M*H$^+$ − H$_2$O 25%]; EI: 303 [*M*$^+$, 10%], 261 [33%], 218 [8%], 148 [10%], and 119 [100%]
M10 (285)		DCI (CH_4): 286 [*M*H$^+$, 100%], and 314 [*M*C$_2$H$_5^+$, 20%]; EI: 285 [*M*$^+$, 9%], 243 [12%] 202 [15%], 174 [20%], and 119 [100%]
M11 (233)	8.15 [d, 1H, Ring C], 8.05 [d, 1H, Ring C], 7.60 [d, 1H, Ring C], 3.90 [s, 3H, OCH$_3$], 3.75 [br s, 2H, CONCH$_2$, Ring D], 3.40 [br s, 2H, CONCH$_2$, Ring D], 1.75 [br s, 4H, Ring D], and 1.60 [br s, 2H, Ring D] (methyl ester)	DCI (CH_4): (methyl ester) 248 [*M*H$^+$, 100%], and 276 [*M*C$_2$H$_5^+$, 8%]; EI: 247 [*M*$^+$, 25%], 246 [74%], 216 [4%], and, 163 [100%]; FAB (thioglycerol): 234 [*M*H$^+$, 100%]
M12 409 (233 + Glu)	7.95 [d, 1H, Ring C], 7.85 [s, 1H, Ring C], 7.45 [d, 1H, Ring C], 3.65 [br s, 2H, CONCH$_2$, Ring D], 3.30 [br s, 2H, CONCH$_2$, Ring D], 1.75 [br s, 4H, Ring D], and 1.60 [br s, 2H, Ring D]	DCI (CH_4): 248 [*M*H$^+$, 100%], and 276 [*M*C$_2$H$_5^+$, 8%]; EI: 247 [*M*$^+$, 25%], 246 [74%], 216 [4%], and, 163 [100%] (sample converted to methyl ester)

Table 3 (*Continued*)

Species[a] (molecular weight, amu)	^{1}H NMR[b], 400 MHz, chemical shifts (δ) ppm (CH_3OH)	*m/z* [cation, % relative intensity]
M13 (235)		DCI (CH_4): 236 [MH^+, 100%], 264 [$MC_2H_5^+$, 18%] and 218 [$MH^+ - H_2O$ 80%]; EI: 235 [M^+, 10%], 234 [35%], and 135 [100%]
M14 (353)	7.40 [m, 3H, Ring C], 7.35 [d, 1H, Ring C], 6.95 [m, 4H, Ring A], 4.55 [m, 1H, $OCH(Me)_2$], 3.60 [s, 2H, NCH_2Ar], 3.15 [br s, 4H, Ring B], 2.60 [br s, 4H, Ring B], and 1.25 [d, 6H, $(Me)_2$]	DCI (CH_4): 354 [MH^+, 70%], and 382 [$MC_2H_5^+$, 5%]; EI: 353 [M^+, 9%], 189 [12%], 176 [15%], 164 [54%] and 134 [100%]
M15 (311)	7.45 [m, 3H, Ring C], 7.35 [d, 1H, Ring C], 7.05 [m, 4H, Ring A], 3.70 [s, 2H, NCH_2Ar], 3.15 [br s, 4H, Ring B], and 2.60 [br s, 4H, Ring B]	DCI (CH_4): 312 [MH^+, 70%], and 340 [$MC_2H_5^+$, 5%]; EI: 311 [M^+, 9%], 147 [18%], and 134 [100%]

[a] See Fig. 1 for Mz numbering scheme.
[b] s = singlet, d = doublet, dd = doublet of doublets, br = broad, and m = multiplet.

and 100 μg with purity between 70 and 90% as determined by NMR. The compounds were dissolved in deuterated methanol-d_4 (CD_3OD) in 5 mm tubes. The chemical shifts (δ) measured in parts-per-million (ppm) were referenced internally to tetramethylsilane.

2.6. Metabolite isolation and identification

Following sample purification, individual metabolites were isolated using column chromatography and HPLC peak collection methods. Unresolved column fractionation residues or HPLC metabolite peaks were further separated using TLC zone scraping methods. The TLC and HPLC procedures were identical to those outlined above. All metabolites were characterized by DCI, and EI MS (Table 3). FAB MS data was obtained only for M11. Proton (^{1}H) NMR data was collected for Mz and for all metabolites except M10, M13 and M5.

2.7. Enzymatic digestion of conjugates and diazomethane derivatization

Conjugates were isolated and purified by HPLC methods described above. Aliquots of dissolved fractions were evaporated to dryness under N_2 gas and adjusted to pH 5.1 with glacial acetic acid and buffered with 1 M sodium acetate. After addition of 100 μL Glusulase®, the mixtures were incubated overnight at 37 °C. The Glusulase® hydrolysis of the glucuronides was inhibited by addition of saccharo-1, 4-lactone. The sulfatase activities were selectively inhibited by incubation in 0.2 M sodium phosphate buffer, pH 6.6. The de-conjugation products were isolated and purified by reversed phase HPLC analysis. Metabolites M5 and M12 were glucuronide conjugates of M4 and M11, respectively (Table 3).

Methyl derivatization of metabolites was performed in the following manner [11]. Metabolites were dissolved in methanol and added to ethereal diazomethane, which was generated from Diazald® with 1N methanolic KOH solution. This mixture was allowed to react overnight at room temperature, evaporated to dryness and analyzed. Phenolic and carboxylic metabolites are readily converted to methyl ethers and methyl ester, respectively.

2.8. Pharmacokinetic and statistical analysis

The plasma concentration versus time data of the total radioactivity for Mz was analyzed by a noncompartmental method [12]. The highest observed plasma concentration and its corresponding sampling time were defined as C_{max} and T_{max}, respectively. The area under the curve (AUC) from time zero to the last sampling time point was calculated by the trapezoidal method. The terminal half-life ($t_{1/2}$) was estimated by a linear regression analysis of the final five data points of the terminal linear segment of the log plasma concentration versus time curve. The Student's *t*-test was used to determine a significant difference between male and female groups with $P = 0.05$ as the minimal level of significance [13].

3. Results and discussion

The total radioactivity, unchanged ^{14}C Mz, and its metabolites (M1–M15) were measured in pooled samples of plasma, urine, and feces for rats (Table 1). For plasma sample pools, the numbers are expressed as the percent of total radioactivity in the sample, since the percent of dose values could not be calculated. The total percent of radioactivity in each sample pool represented by identified metabolites are also listed Table 1. The percent values were obtained by peak area integration of radiochromatograms (data not shown). In general, these peak areas had a coefficient of variation and accuracy within 15% if the areas were >5% of the dosed sample. Peak areas accounting for <5% of the radioactivity in a sample are represented by a plus sign. The negative sign in Table 1 indicated that the metabolite was not detected above approximately 2 ng equiv./mL. The percent of administered dose excreted in urine and fecal extract and the percent of sample represented by each metabolite in plasma, urine and fecal extract pools are summarized at the bottom of Table 1. In general, >80% of the radioactivity in plasma, urine and fecal extracts has been accounted for by identified metabolites. Mz accounted for approximately 8% of the radioactivity in plasma and <5% in the other excreta samples. These data indicated that Mz was extensively metabolized after oral administration to rats.

The recovery of total radioactivity in urine and feces was determined for mass balance considerations and to examine gen-

der differences. The cumulative radioactivity in urine (0–168 h) and feces (0–168 h) was not significantly different ($P > 0.05$) between male and female rats. In the 7 days following the oral administration of ^{14}C Mz, the mean recovery of total radioactivity was 92.5 ± 4.1% of the dose, 30.0 ± 2.1% of the dose was excreted in urine and 62.6 ± 5.6% in the feces. In addition, the rate of disposition of Mz and its metabolites was rapid. Approximately 94% of the total urinary radioactivity and approximately 81% of the total fecal radioactivity was excreted within 24 h after oral dosing.

The maximal plasma concentration (C_{max}) of total radioactivity and unchanged Mz in male and female rats were measured and both occurred at approximately 0.5 h (T_{max}) after oral administration of ^{14}C Mz (Table 2 and Fig. 1). The C_{max}, and the AUC (0–24 h) values were consistently higher in the female rats. In both male and female rats the percentage of Mz in the AUC represented only a small portion of the total AUC. From Table 2, it was estimated that approximately 2% of the total radioactivity in male rats was attributed to unchanged Mz while 8% was estimated for female rats. The total radioactivity in male and female rats displayed a considerably long terminal half-life (9–13 h) when compared to unchanged Mz (1–2 h). These results indicate that Mz is rapidly eliminated following oral administration to rats.

Unchanged Mz and a total of 15 metabolites (M1–M15) were isolated from plasma, urine and feces samples. The structure of Mz and these 15 metabolites were tentatively identified based on a variety of chromatographic and spectroscopic techniques (Fig. 2). The proton (^{1}H) NMR chemical shifts (ppm) and the MS fragments (*m/z*) for Mz and the isolated metabolites (M1–M15) are presented in Table 3.

Unchanged Mz was isolated from plasma by TLC and HPLC methods. It was identified on the basis of HPLC, MS and NMR data (Table 3) in comparison with those data obtained from an authentic Mz sample [9]. The DCI analysis of this isolated material revealed a significant protonated molecular cation [MH$^+$] at *m/z* 422. This MS data verified the molecular weight of 421 Da for Mz. The EI spectra contained many characteristic fragment cations with the majority of these cations occurring from fragmentation around the piperazine ring. An EI MS fragmentation scheme is shown in Fig. 3 to facilitate the interpretation of the EI data. This fragmentation scheme can be used to approximately locate oxidation sites on the four ring systems (A–D) of Mz. For example, *m/z* 176 and 164 cations contains information about the A aromatic ring system (i.e. Ring A) while *m/z* 257 and 230 cations contain information about Rings B–D. The *m/z* 202 cation contains information about Rings C and D and *m/z* 119 cation contains information about Ring C. The ^{1}H NMR spectrum of isolated Mz and the reference compound were compared (data not shown). Based on coupling constants and chemical shift arguments the spectrum was assigned as follows. The aromatic protons (Rings A and C) were located between δ 8 and 7 ppm (Table 3). The four protons on Ring A were centered at δ 6.9 ppm. Ring C protons were centered at δ 7.45 (three protons) and 7.25 ppm (one proton). These protons can be used readily to elucidate the substitution pattern on these aromatic ring systems. The multiplet resonance centered at δ 4.6 ppm, which integrated for one proton, was assigned to the OCH proton on the isopropyl group. The methyl protons of the isopropyl group were assigned to a single resonance centered at δ 1.25 ppm, which integrated for six protons. The multiplet resonances centered at δ 3.75 and 3.45 ppm, each integrating for two protons, were assigned to the *N*-methylene protons on the piperidine ring (Ring D). The multiplet resonances centered at δ 1.75 and 1.55 ppm, both integrating for a total of six protons, were assigned to the aliphatic protons on the piperidine ring (Ring D). The multiplet resonances centered at δ 3.10 and 2.65 ppm, each integrating for four protons, were assigned to the *N*-methylene protons on the piperazine ring (Ring B). The singlet resonance centered at δ 3.6 ppm, which integrated for two protons, was assigned to the *N*-methylene protons between Rings A and B. The chromatographic and spectroscopic data for this isolated sample was identical to those of the synthetic sample RWJ-37796 [9].

Metabolite M1 was isolated from feces by TLC and HPLC methods. The identification of M1 was performed on the basis of the MS, NMR and comparison with an authentic sample of M1 (RWJ-50503) [9]. The DCI spectrum of M1 revealed a protonated molecular cation [MH$^+$] at *m/z* 438, which was 16 Da higher than the MH$^+$ of Mz. This MS data suggested a molecular weight of 437 Da for M1. Comparison of the EI data from Mz and M1 revealed prominent cations at *m/z* 192 (176 + 16) and at *m/z* 180 (164 + 16). Using the fragmentation scheme in Fig. 3, these shifts in *m/z* when comparing Mz to M1 suggested that the oxidation in M1 had occurred on the Ring A. ^{1}H NMR data revealed that M1 contained one less aromatic proton on Ring A consistent with the MS data. The aromatic proton pattern (i.e. chemical shifts and coupling constants) of the three remaining protons on Ring A suggested that the *para*-position relative to the piperazine ring had been hydroxylated (Fig. 2). M1 was further derivatized to a methyl ether analog by ethereal diazomethane. MS and NMR data of this derivative were consistent with this para assignment.

Metabolite M2 was isolated from plasma and identified using MS, NMR and comparison with an authentic sample of M2 (RWJ-48772) [9]. The DCI spectrum of M2 revealed a protonated molecular cation [MH$^+$] at *m/z* 438, which was 16 Da higher than the MH$^+$ of Mz. This MS data suggested a molecular weight of 437 Da for M2. Comparison of the EI data from Mz and M1 revealed prominent cations at *m/z* 273 (257 + 16), *m/z* 246 (230 + 16) and at *m/z* 218 (202 + 16). Using the fragmentation scheme in Fig. 3, these shifts in *m/z* when comparing Mz to M2 suggested that the oxidation in M2 had occurred on the Ring D. ^{1}H NMR data revealed that M2 contained one less proton on Ring D consistent with the MS data. The aliphatic proton NMR shift pattern on Ring D suggested that the four position of piperidine ring system had been hydroxylated (Fig. 2). M2 could not be further derivatized to a methyl ether analog by ethereal diazomethane. The chromatographic and spectroscopic data for M2 were identical to those of synthetic sample RWJ-48772 [9].

Metabolite M3 was isolated from feces and identified using MS, and NMR techniques. The MS DCI spectrum of M3 revealed a protonated molecular cation [MH$^+$] at *m/z* 454, which was 32 Da higher than the MH$^+$ of Mz. This MS data suggested a molecular weight of 453 Da for M2. Comparison of the EI data

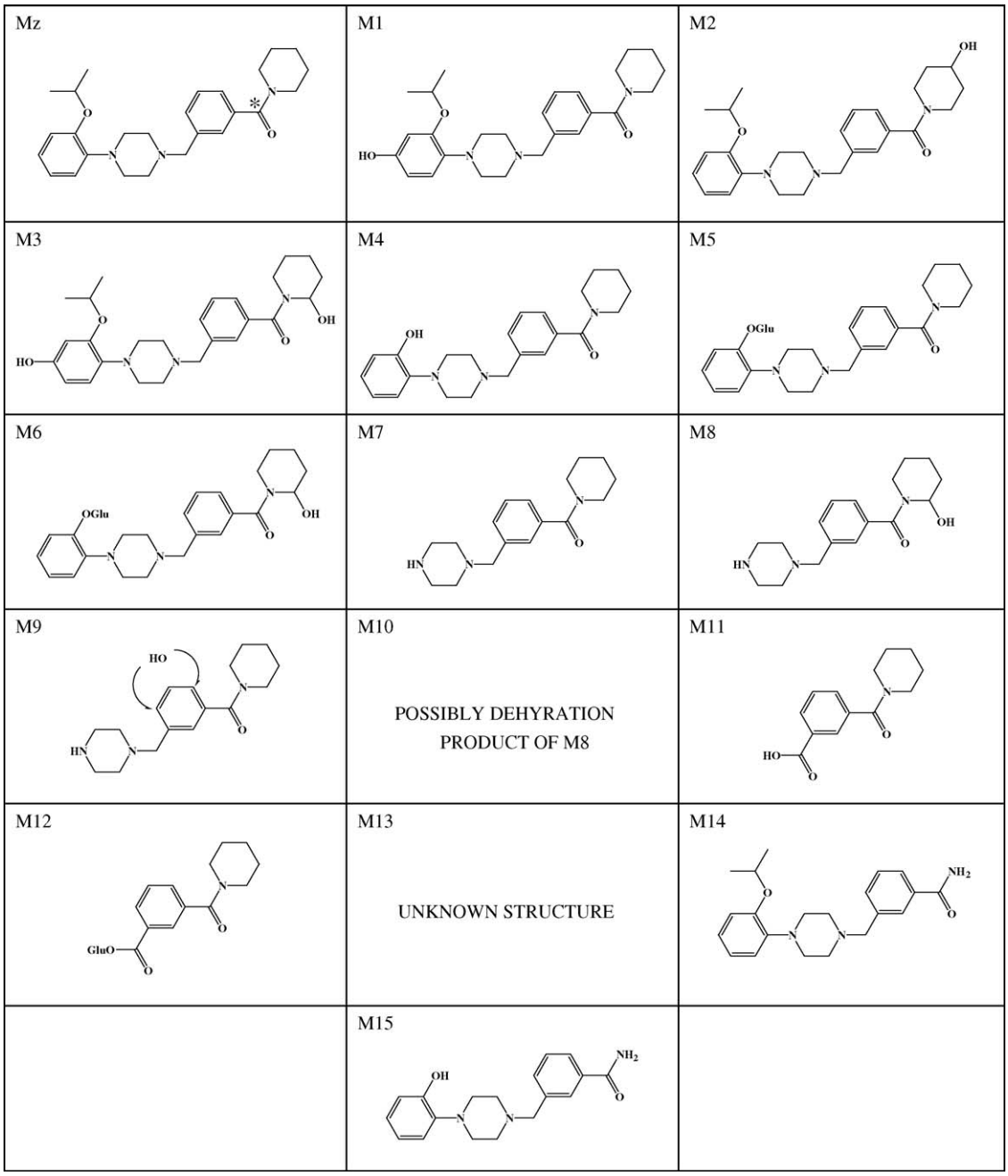

Fig. 2. Structures of mazapertine (Mz) and its metabolites in rats. The asterisk for Mz indicates the position of the ^{14}C label. The abbreviation Glu denotes β-D-glucuronic acid. Metabolites M1 (RWJ-50503), M2 (RWJ-48772), M4 (RWJ-50292), M7 (RWJ-47999), M11 (RWJ-48278) and M14 (RWJ-38037) were prepared synthetically to validate structural assignments (Ref. [9]).

from Mz, M1 and M2 with M3 revealed prominent cations at *m/z* 246 (230 + 16), *m/z* 218 (202 + 16), *m/z* 192 (176 + 16), and *m/z* 180 (176 + 16). Using the fragmentation scheme in Fig. 3, these shifts in *m/z* suggested that the oxidation in M3 had occurred on both Rings A and D. ^{1}H NMR data revealed that M3 contained one less aromatic proton on Ring A consistent with the MS data. The aromatic proton pattern of the three remaining protons on Ring A suggested that the *para*-position relative to the piperazine ring had been hydroxylated. ^{1}H NMR data revealed that M3 contained one less proton on Ring D consistent with the MS data. The proton resonance at δ 4.2 ppm, which integrated for one proton, suggested that the *N*-methylene position on Ring D had been hydroxylated (Fig. 2).

Metabolite M4 was isolated from plasma and identified using MS, NMR and comparison with an authentic sample of M4 (RWJ-50292) [9]. The MS DCI spectrum of M4 revealed a protonated molecular cation [MH$^+$] at *m/z* 380, which was 42 Da lower than the MH$^+$ of Mz. This MS data suggested a molecular weight of 379 Da for M4. Comparison of the EI data from Mz and M1 revealed prominent cations at *m/z* 257, and *m/z* 134 (176 − 42). Using the fragmentation scheme in Fig. 3, these shifts in *m/z* suggested that M4 was the desisopropyl analog of

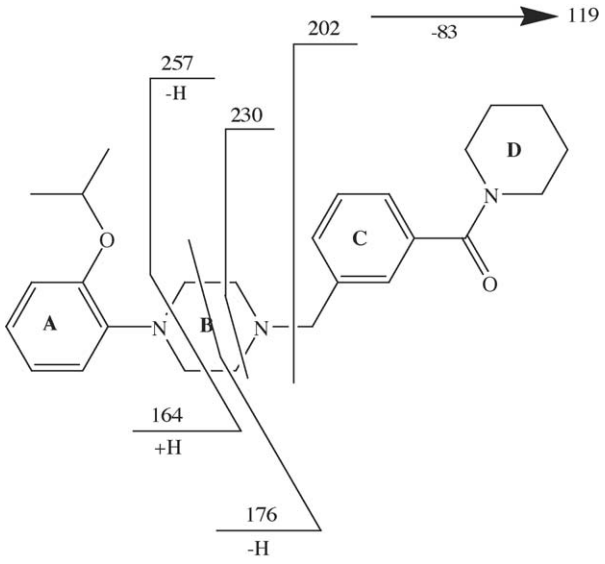

Fig. 3. Structure of mazapertine (1-[3-[[4-[2-(1-methylethoxy)phenyl]-1-piperazinyl]methyl]benzoy]piperidine succinate (RWJ-37796, Mz)). The most prominent EI MS cations are generated from fragmentation of the piperazine ring.

Mz. ^{1}H NMR data revealed the absence of the isopropyl group consistent with the MS data. M4 was further derivatized to a methyl ether analog by ethereal diazomethane. The chromatographic and spectroscopic data (Fig. 4) for M4 were identical to those of synthetic sample RWJ-50292 [9].

Metabolite M5 was isolated from feces and identified as the glucuronic conjugate of M4. The EI and the DCI mass spectrum of M5 were identical to M4 suggesting that the M5 conjugate had decomposed in the mass spectrometer back to M4. ^{1}H NMR data revealed that M5 was very similar to M4; however, the NMR spectrum of M5 contained proton sugar resonances suggesting

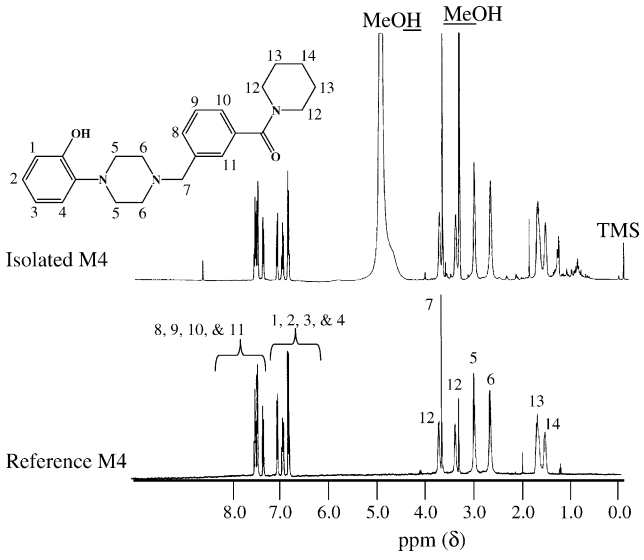

Fig. 4. Structures of metabolite M4 (1-[3-[[4-[2-(hydroxy)phenyl]-1-piperazinyl]-methyl]benzoy]piperidine succinate (RWJ-50292)) and numbering scheme. ^{1}H NMR spectra of M4 isolated from rat feces and synthetic sample of M4 (Ref. [9]).

the presence of a β-D-glucuronic conjugate [14]. Glusulase® hydrolysis experiments were consistent with this assignment.

Metabolite M6 was isolated from feces and identified using MS, NMR, and Glusulase® hydrolysis techniques as a glucuronic conjugate. The MS DCI spectrum of M6 revealed a protonated molecular cation [MH$^+$] at m/z 396. This MS data suggested a molecular weight of 395 Da for M6. Comparison of the EI data from Mz, and M1–M4 suggested that oxidation in M6 had occurred on Ring D and the isopropyl group was no longer present. ^{1}H NMR data revealed that the isopropyl group in Ring A was absent and that Ring D had been hydroxylated; however, the exact position of hydroxylation on the piperidine ring could not be determined. The aromatic chemical shifts in Ring A of M5 and M6 were identical. The NMR spectrum of M6 also contained proton sugar resonances suggesting the presence of a β-D-glucuronic conjugate [14]. Based on the NMR results, it was concluded that M6 was probably a glucuronic conjugate and had decomposed in the mass spectrometer losing its sugar moiety in a similar fashion to M5. Glusulase® hydrolysis experiments were consistent with this argument and the assignment of M6.

The identification of M7 was performed on the basis of the MS, NMR and comparison with an authentic sample of M7 (RWJ-47999) [9]. M7 was isolated from urine. The MS DCI spectrum of M7 revealed a protonated molecular cation [MH$^+$] at m/z 288. This MS data suggested a molecular weight of 287 Da for M7. Comparison of the EI data from Mz and M7 and using the fragmentation scheme in Fig. 3, suggested that M7 was the N-debenzylation analog of Mz (Fig. 2). ^{1}H NMR data confirmed that Ring A was absent which was consistent with the MS data (Table 3). The chromatographic and spectroscopic data for M7 were identical to those of the synthetic sample RWJ-477999 [9].

Metabolite M8 was identified using MS and NMR techniques. The MS DCI spectrum of M8 revealed a protonated molecular cation [MH$^+$] at m/z 304, which was 16 Da higher than the MH$^+$ of M7. This MS data suggested a molecular weight of 303 Da for M8. Comparison of the EI data from M7 with M8 revealed a prominent cation at m/z 245 and m/z 261, respectively. Based on these data, it was speculated that the loss of the fragment NCH_2CH_2 group (42 Da) from the piperazine ring (Ring B) could account for both cations. For example, the m/z 245 cation in the EI spectrum of M7 could arise from the loss of 42 Da from 287. Using the same argument, the m/z 261 cation in the EI spectra of M8 could arise from the loss of 42 Da from 303. These shifts in m/z suggested that the oxidation in M8 had occurred on either Rings C or D. ^{1}H NMR data revealed that Ring A was absent in M8. In addition, the NMR data contained one less proton on Ring D consistent with the MS data. The proton resonance centered at δ 4.2 ppm, which integrated for one proton, suggested that the N-methylene position on Ring D had been hydroxylated (Fig. 2).

Metabolite M9 was identified using MS, and NMR techniques. The DCI spectrum of M9 revealed a protonated molecular cation [MH$^+$] at m/z 304, which was 16 Da higher than the MH$^+$ of M7 and the same as M8. This MS data suggested a molecular weight of 303 Da for M9. Comparison of the EI data from M8 with M9 revealed no prominent differences to suggest

the location of the hydroxylation. ^{1}H NMR data revealed that M9 contained one less aromatic proton on Ring C. However, the exact position of the hydroxylation on Ring C could not be determined (Fig. 2).

The structure of metabolite M10 was tentatively proposed on the basis of only MS data. Due to chromatographic and EI fragmentation similarities between M7 and M10, the structure was suggested as the dehydrated product of M9. Further structural confirmation of this metabolite was terminated because of insufficient material for NMR analysis.

The identification of M11 was performed on the basis of the MS, NMR, derivatization techniques and comparison with an authentic sample of M11 (RWJ-48278) [9]. A significant amount of M11 was found in plasma and urine. The isolated material did not exhibit any DCI adduct cations or any significant EI fragments; however, the FAB spectrum showed a molecular sodium molecular adduct cation at *m/z* 256 (MNa^{+}) and its corresponding protonated molecular cation at *m/z* 234 (MH^{+}). This MS data suggested that the molecular weight of M11 was 233 Da. Since the isolated material was too unstable to obtain spectroscopic data, it was derivatized using an excess of ethereal diazomethane. The derivatized product showed an intense protonated molecular cation at *m/z* 248. Comparison of the original FAB data of the isolated material and the DCI data of the derivatized material suggested a single methyl group had been added to the isolated material. ^{1}H NMR data confirmed that the methyl ester of M11 was produced during the derivatization procedure. The chromatographic and spectroscopic data for the methyl ester of M11 were identical to those of the synthetic sample RWJ-477999 [9].

Metabolite M12 was isolated from urine and identified as the glucuronic conjugate of M11. The EI and the DCI mass spectrum of M12 were identical to M11; however, the chromatographic results showed that M12 was more polar when compared to M11. These data suggested that the M12 conjugate had decomposed in the mass spectrometer back to M11. ^{1}H NMR data revealed that M12 was very similar to M11. The NMR spectrum of M12 also contained proton sugar resonances suggesting the presence of a β-D-glucuronic conjugate [14]. After Glusulase® hydrolysis followed by Diazald® treatment, the MS and NMR of M12 were identical to M11.

Metabolite M13 was isolated in a very minor amount from urine and its exact structure could not be determined. The DCI spectrum of M13 revealed a protonated molecular cation [MH^{+}] at *m/z* 236. This MS data suggested a molecular weight of 235 Da for M13. The EI spectrum showed few prominent cations for structural elucidation. The chromatographic results showed that M13 was much less polar than M11. In addition, M13 could not be further derivatized to a methyl derivative using ethereal diazomethane. These data suggested that M13 was not a carboxylic acid. Further structural confirmation of this metabolite was terminated because of insufficient material for NMR analysis.

Metabolite M14 was isolated from urine by TLC and HPLC methods. The identification of M14 was performed on the basis of the MS, NMR and comparison with an authentic sample of M14 (RWJ-38037) [9]. The DCI spectrum of M14 revealed a protonated molecular cation [MH^{+}] at *m/z* 354. This MS data suggested a molecular weight of 353 Da for M14. Comparison of the EI data from Mz and M14 revealed prominent cations at *m/z* 164 and 176 suggesting that Ring A was present; however, the *m/z* 134 cation suggested that Ring D was absent. ^{1}H NMR data confirmed that Ring D was absent which was consistent with the MS data (Table 3). The chromatographic and spectroscopic data for M14 were identical to those of the synthetic sample RWJ-38037 [9].

Metabolite M15 was isolated from urine and identified using MS, NMR and derivatization techniques. The DCI spectrum of M15 revealed a protonated molecular cation [MH^{+}] at *m/z* 312, which was 42 Da lower than the MH^{+} of M14. This MS data suggested a molecular weight of 311 Da for M15. Comparison of the EI data from M14 and M15 revealed prominent cations at *m/z* 134 and *m/z* 147 (189 − 42). These shifts in *m/z* suggested that M15 was the desisopropyl analog of M14. ^{1}H NMR data revealed the absence of the isopropyl group consistent with the MS data. M15 was further derivatized to a methyl ether analog by ethereal diazomethane.

4. Conclusion

The drug disposition of mazapertine has been investigated in male and female Sprague–Dawley rats. Rats received an orally administered radioactive dose (30 mg/kg) of Mz. The absorption of Mz was rapid since the maximal plasma concentration of Mz and total radioactivity occurred at 0.5 h after dosing. The Mz concentration declined rapidly in plasma with a terminal half-life <2 h whereas the total radioactivity displayed a considerably longer terminal half-life of 9–13 h. The cumulative (7 days) radioactivity recovery of Mz was 93% with fecal elimination accounting for approximately 63% of the dose and urine accounting for 30%. There were no significant gender differences in the overall excretion pattern. Mz and a total of 15 metabolites were isolated and identified in these samples. Six proposed pathways were used to describe the formation of the metabolites of Mz (Fig. 2): (1) phenyl hydroxylation, (2) piperidyl oxidation, (3) *O*-dealkylation, (4) *N*-dephenylation, (5) oxidative *N*-debenzylation and (6) glucuronide conjugation. Unchanged Mz accounted for <5% of the radioactive dose in excreta samples and <8% of the sample in plasma (0–24 h). The most dominant metabolism pathway of Mz appeared to be phenyl hydroxylation to form metabolite M1 (Fig. 2), piperidine hydroxylation to form M2, *O*-dealkylation to form M4, and oxidative *N*-debenzylation to form M11. It appeared that rats metabolized Mz more extensively than humans [4].

Acknowledgements

The authors thank Dr. L.E. Weaner for synthesizing [^{14}C] Mz. We thank A.R. Takacs, S.L. Vaughn, and J.A. Buben for important contributions to this effort.

References

[1] A.B. Reitz, D.J. Bennett, P.S. Blum, E.E. Codd, C.A. Maryanoff, M.E. Ortegon, M.J. Renzi, M.K. Scott, R.P. Shank, J.L. Vaught, J. Med. Chem. 37 (1994) 1060–1062.

[2] A.B. Reitz, M.K. Scott, in: B.E. Maryanoff, C.A. Maryanoff (Eds.), Advances in Medicinal Chemistry, vol. 3, JAI, Greenwich, Conn., 1995, pp. 1–56.
[3] A.B. Reitz, E.W. Baxter, E.E. Codd, C.B. Davis, A.D. Jordan, B.E. Maryanoff, C.A. Maryanoff, M.E. McDonnell, E.T. Powell, M.J. Renzi, M.R. Schott, M.K. Scott, R.P. Shank, J.L. Vaught, J. Med. Chem. 41 (1998) 1997–2009.
[4] T. Buclin, R. Stucki, F. Jaquet-Mueller, A. Munafo, C. Bauldauf, F. Brunner-Ferber, J. Biollaz, Clin. Pharmacol. Ther. 53 (1993) 179 (abstract, 94th Annual Meeting of the American Society for Clinical Pharmacology and Therapeutics).
[5] L.G. Gisclon, C.R. Curtin, Pharmaceut. Res. 10 (1993) S-398 (abstract, the 8th AAPS Annual Meeting).
[6] W.N. Wu, L.A. McKown, A.B. Reitz, Eur. J. Drug Metab. Pharm. 28 (2003) 279–286.
[7] W.N. Wu, L.A. McKown, A.R. Takacs, W.J. Jones, A.B. Reitz, Xenobiotica 29 (1999) 453–466.
[8] W.N. Wu, L.A. McKown, Cur. Drug Metab. 1 (2000) 255–270.
[9] A.B. Reitz, M.E. McDonnell, E.W. Baxter, E.E. Codd, W.N. Wu, Bioorg. Med. Chem. Lett. 7 (1997) 1927–1930.
[10] E.W. Baxter, A.B. Reitz, Bioorg. Med. Chem. Lett. 7 (1997) 763–768.
[11] W.N. Wu, L.A. McKown, in: Z. Yan, G.W. Caldwell (Eds.), Optimization in Drug Discovery, Humana Press, Totowa, New Jersey, 2004, pp. 163–184.
[12] M. Gibaldi, D. Perrier, Pharmacokinetics, Marcel Dekker Inc., New York and Basel, 1982.
[13] J.C. Miller, J.N. Miller, Statistics for Analytical Chemistry, 2nd ed., Ellis Hardwood Limited, West Sussex, England, 1992.
[14] G.C. Leo, W.N. Wu, J. Pharm. Biomed. Anal. 10 (1992) 607–613.